

# Unexpected drop of dynamical heterogeneities in colloidal suspensions approaching the jamming transition

Pierre Ballesta<sup>1,2</sup>, Agnès Duri<sup>1,3</sup>, and Luca Cipelletti<sup>1\*</sup>

<sup>1</sup>*LCVN UMR 5587, Université Montpellier 2 and CNRS,  
34095 Montpellier Cedex 5, France*

<sup>2</sup> *Present Address: HASYLAB at DESY, D-22603 Hambourg, Germany*

<sup>3</sup> *Present address: School of Physics,  
The University of Edinburgh, Edinburgh EH9 3JZ, UK\**

(Dated: November 1, 2021)

## Abstract

As the glass (in molecular fluids[1]) or the jamming (in colloids and grains[2]) transitions are approached, the dynamics slow down dramatically with no marked structural changes. Dynamical heterogeneity (DH) plays a crucial role: structural relaxation occurs through correlated rearrangements of particle “blobs” of size  $\xi$ [3, 4, 5, 6]. On approaching these transitions,  $\xi$  grows in glass-formers[5, 6], colloids[3, 7], and driven granular materials[8] alike, strengthening the analogies between the glass and the jamming transitions. However, little is known yet on the behavior of DH very close to dynamical arrest. Here, we measure in colloids the maximum of a “dynamical susceptibility”,  $\chi^*$ , whose growth is usually associated to that of  $\xi$ [9].  $\chi^*$  initially increases with volume fraction  $\varphi$ , as in[8], but strikingly drops dramatically very close to jamming. We show that this unexpected behavior results from the competition between the growth of  $\xi$  and the reduced particle displacements associated with rearrangements in very dense suspensions, unveiling a richer-than-expected scenario.

PACS numbers: 61.43.Fs Glasses, 64.70.Pf Glass transitions, 82.70.Dd Colloids, 83.80.Hj Suspensions, dispersions, pastes, slurries, colloids

---

\*Electronic address: lucacip@lcvn.univ-montp2.fr

The recent observation of a critical-like growth of temporal and spatial dynamical fluctuations in a 2D athermal system approaching jamming[8], similar to that hypothesized for glass formers[10], has raised hope that the glass and the jamming transition may be unified, calling at the same time for further, tighter experimental verifications. Here, we investigate temporal DH in a 3D thermal system, concentrated colloidal suspensions close to the maximum packing fraction. Temporal and spatial DH are usually closely related: the former can be quantified by a “four-point dynamical susceptibility”  $\chi_4$  (the variance of a time-resolved correlation function describing the system relaxation), whose amplitude is proportional to  $\xi^3$ [9, 11, 12]. Surprisingly, we find that very close to jamming temporal and spatial DH decouple: while  $\xi$  continuously grows with volume fraction, the amplitude of temporal fluctuations drops sharply close to the maximum packing fraction. These findings challenge current scenarios where the slowing down of the dynamics on approaching jamming is accompanied by enhanced dynamical fluctuations.

We study concentrated suspensions of polyvinylchloride (PVC) xenospheres[13] suspended in dioctylphthalate (DOP). The particles are highly polydisperse, with typical diameter  $\approx 10 \mu\text{m}$ ; they behave as slightly deformable hard spheres. The samples are loaded in cells of thickness  $L = 2 \text{ mm}$ , vigorously stirred and outgassed to remove air bubbles. The dynamics are probed by dynamic light scattering in the highly multiple scattering limit (Diffusing Wave Spectroscopy, DWS[14]), adopting the transmission geometry, with  $L/\ell^* \approx 10$ , where  $\ell^*$  is the photon transport mean path. This technique allows the dynamics to be probed on length scales as small as a few nm[14], which match well the restrained motion in tightly packed suspensions. A charge-coupled-device (CCD) detector is used to record the speckle pattern scattered by the sample. The evolution of the speckle images is quantified by the two-time degree of correlation[15]  $c_I(q, t, \tau) = \langle I_p(t)I_p(t + \tau) \rangle_p / \left( \langle I_p(t) \rangle_p \langle I_p(t + \tau) \rangle_p \right) - 1$ , where  $I_p(t)$  is the scattered intensity at pixel  $p$  and time  $t$  and  $\langle \dots \rangle_p$  is an average over the CCD pixels.

In order to follow the evolution of the dynamics, we calculate  $g_2(t, \tau) - 1$ , the two-time intensity correlation function obtained by averaging  $c_I(t, \tau)$  over a few CCD frames. Due to the limited acquisition rate of the CCD, the initial decay of  $g_2(t, \tau) - 1$  is not captured; at longer delays, a plateau followed by a final relaxation is observed (see Fig. 2a for an example of a time-averaged  $g_2$ ), indicative of very slow rearrangements. Figure 1a shows a typical example of the time dependence of  $\tau_0$ , the characteristic time of the final relaxation obtained

by fitting  $g_2 - 1$  to a stretched exponential  $a(t) \exp \left\{ - [\tau/\tau_0(t)]^{\beta(t)} \right\}$ . Initially,  $\tau_0$  grows nearly linearly with  $t$ , as observed in many glassy systems. However, for  $t > 28000$  sec a stationary regime is observed, where  $\tau_0$  exhibits surprisingly large fluctuations but no overall increasing trend. A similar behavior is observed for all volume fractions; all data presented in the following refer to the stationary regime[16]. We first investigate the  $\varphi$ -dependence of the average dynamics, as quantified by  $\overline{\tau_0}$  and  $\overline{\beta}$ , where  $\overline{\dots}$  denotes a time average. As shown in Fig. 1b,  $\overline{\tau_0}$  continuously increases with  $\varphi$ . Data taken for freshly prepared samples (solid circles) can be fitted by a critical law,  $\overline{\tau_0} \sim 1/|\varphi/\varphi_{\max} - 1|^x$ , with  $\varphi_{\max} = 0.752$ , consistent with expectations for highly polydisperse samples[17], and  $x = 1.01 \pm 0.04$ , similarly to Ref.[8]. We also study samples that have been aged for several days and whose dynamics is re-initialized by vigorously stirring and outgassing them (semi-open circles). Their effective volume fraction is higher than the nominal one, due to the slight swelling of PVC particles suspended in DOP for very long times[13], allowing to achieve an even tighter packing. To compare the dynamics of both fresh and aged samples, we assign an effective volume fraction,  $\varphi_{\text{eff}}$ , to the latter so that their average relaxation time falls on the critical-like curve determined for the fresh samples. Figure 1c shows  $\overline{\beta}(\varphi)$ : at the lowest volume fraction, the shape of  $g_2$  is slightly stretched ( $\overline{\beta} = 0.86 < 1$ ), similarly to what observed for correlation functions in many glassy systems[1]. Surprisingly, as  $\varphi$  increases  $\overline{\beta}$  grows above one, finally saturating around 1.3. A similar ‘‘compressed’’ exponential relaxation has been observed in single [18, 19, 20] and multiple[21, 22] scattering experiments on systems close to jamming, usually associated with ultra-slow ballistic motion.

We quantify the temporal fluctuations of the dynamics by calculating  $\chi(\tau, \varphi)$ , the relative variance of  $c_I$ , defined by

$$\chi(\tau) \equiv \chi(\tau, \varphi) = \overline{\left( c_I(t, \tau) - \overline{c_I(t, \tau)} \right)^2} / \overline{c_I}^2, \quad (1)$$

where the normalization is introduced to account for the  $\varphi$ -dependence of the amplitude of the final relaxation of  $g_2 - 1$ ; data are furthermore corrected for experimental noise[15]. The variance introduced above corresponds to the dynamical susceptibility  $\chi_4$  much studied in simulations of glass formers [9, 11, 23]. Figure 2a shows both the average correlation function  $\overline{g_2} - 1$  (open circles) and  $\chi$  (solid circles) for  $\varphi = 0.738$ . The dynamical susceptibility exhibits a marked peak around  $\tau_0$ , a direct manifestation of DH also found in many other glassy systems[4, 8, 9, 11, 12, 24].

Figure 2b shows the height of the peak of the dynamical susceptibility,  $\chi^*$ , as a function of  $\varphi$ . At the lowest volume fractions,  $\chi^*$  increases with  $\varphi$ ; the data can be fitted by a critical law  $\chi^* \sim 1/|\varphi/\varphi_{\max} - 1|^y$  with  $y = 1.5 \pm 0.2$  (line in Fig. 2b), close to  $y = 1.70$  recently reported for driven grains[8]. This growing trend is also analogous to that observed in simulations of glass formers[5] and colloids[3, 7] (albeit at lower  $\varphi$ ) and has been interpreted as due to a growing dynamical length scale on approaching dynamical arrest. At higher volume fractions, however, an opposite trend is observed: the amplitude of dynamical fluctuations dramatically decreases close to  $\varphi_{\max}$ . This striking behavior represents our central result, which challenges current views of DH close to dynamical arrest. The unexpected drop of dynamical fluctuations very close to jamming is confirmed by the non-monotonic behavior of the width of the temporal distributions of  $\tau_0$  and  $\beta$ , shown by the vertical bars in Fig. 1b-c. The dispersion of both parameters initially increases with  $\varphi$ , but is eventually reduced close to  $\varphi_{\max}$ , further demonstrating reduced DH.

We propose that the non-monotonic behavior of  $\chi^*$  results from a competition between the growth of  $\xi$  on approaching  $\varphi_{\max}$  and the reduced particle displacement associated with rearrangement events close to jamming, due to tighter packing[25, 26, 27, 28]. Indeed, as  $\xi$  increases, fewer statistically independent dynamical regions are contained in the sample, leading to enhanced fluctuations[24]. Conversely, as particle displacement decreases  $\chi^*$  is reduced, since more events are required to significantly decorrelate the scattered light and fluctuations on a time scale  $\sim \overline{\tau_0}$  tend to be averaged out. These competing mechanisms should be quite general and should be observable in a variety of systems, provided that DH are probed close enough to dynamical arrest.

We have incorporated these ideas in a simple model for DWS for a dynamically heterogeneous process, significantly extending previous work on the intermittent dynamics of foams[29] and gels[30]. The dynamics is assumed to be due to discrete rearrangement events of volume  $\xi^3$  that occur randomly in space and time; however, in contrast to Ref.[29] we assume that several events will be in general necessary to fully decorrelate the phase of scattered photons, since in concentrated suspensions the particle displacement associated with one single event may be much smaller than the wavelength of the light. The two-time field correlation function for a photon crossing the cell along a path of length  $s$  may then be written as

$$g_1^{(s)}(t, \tau) = \exp[-n_s(t, \tau)^p \sigma_\phi^2]. \quad (2)$$

Here,  $n_s(t, \tau)$  is the number of events along the path between time  $t$  and  $t + \tau$  and  $\sigma_\phi^2$  is the variance of the change of phase of a photon due to one single event, related to the particle mean squared displacement associated with such event,  $\sigma^2$ , by  $\sigma_\phi^2 \approx 20\sigma^2/\mu\text{m}^2$ [31]. For a totally uncorrelated change of photon phase due to distinct events one has  $p = 1$ , while in the opposite limit of a perfectly correlated change of phase  $p = 2$ [14].

We implement our model in Monte Carlo simulations where photon paths are random walks on a square lattice with lattice parameter  $\ell^*$ . The lattice sites are affected by random rearrangement events of volume  $\xi^3$ , occurring at a constant rate per unit volume. The simulated degree of correlation is calculated from  $c_{I,\text{sim}}(t, \tau) = \left[ N_s^{-1} \sum g_1^{(s)}(t, \tau) \right]^2$ , where the sum is over  $N_s = 200000$  photon paths and  $g_1^{(s)}$  is calculated according to (2). The two-time intensity correlation function,  $g_{2,\text{sim}}(t, \tau)$ , and its fluctuations,  $\chi_{\text{sim}}$ , are then calculated from  $c_{I,\text{sim}}$  as for the experiments. We vary the control parameters in the simulation,  $\xi^3$ ,  $p$ , and  $\sigma_\phi^2$ [32], to reproduce the experimental  $\varphi$ -dependence of  $\bar{\beta}$  and  $\chi^*$ . Since the particle displacement resulting from one rearrangement —and thus  $\sigma_\phi^2$ — is expected to decrease as  $\varphi$  grows, due to tighter particle packing[25, 26, 27, 28], we choose  $1/\sigma_\phi^2$  as the control parameter against which simulation results are presented, corresponding to increasing volume fractions in Fig. 1b-c). Figure 3a shows  $\bar{\beta}$  vs  $1/\sigma_\phi^2$ . The data are obtained using the values of  $\xi^3$  shown in Fig. 3c; however, we find that  $\bar{\beta}$  depends only very weakly on  $\xi^3$ . For large particle displacements (small  $1/\sigma_\phi^2$ ),  $\bar{\beta} \lesssim 1$  in fair agreement with the experimental value at the lowest  $\varphi$ . As particle displacements become increasingly restrained,  $\bar{\beta}$  grows and saturates at  $\bar{\beta} \approx 1.3$ , close to the experimental values at the highest  $\varphi$ . The saturation value depends on the choice of  $p$ [33]: here,  $p = 1.65$ , showing that the change of phase of a photon due to distinct rearrangements is partially correlated. It is unlikely that such a correlation exists for events occurring in non-overlapping regions; by contrast, successive events in the same region will lead to partially correlated changes of phase when the direction of displacement persists during several events. Thus,  $p = 1.65$  indicates intermittent supradiffusive motion, a behavior close to the ballistic motion reported for many jammed systems[18, 19, 20, 21, 22].

Figure 3b shows the  $1/\sigma_\phi^2$  dependence of  $\chi^*$ . The simulations reproduce well both the non-monotonic trend and the absolute values of the experimental  $\chi^*$ . They reproduce also the non-monotonic  $\varphi$ -dependence of the dispersion of  $\beta$  (bars in Fig. 3a), once again matching closely the experimental data. In spite of the drop of dynamical fluctuations close to  $\varphi_{\text{max}}$ ,  $\xi^3$  grows steadily with  $\varphi$  (Fig. 3c), until rearrangement events span the whole sample,

corresponding to  $\xi \approx 2000$  particle diameters. System-spanning “earthquakes” have been reported in simulations of both thermal[34] and athermal[28] systems close to dynamical arrest, but have never been observed experimentally.

Our results show that the behavior of dynamical heterogeneity very close to the jamming transition is much richer and complex than expected. On the one hand, the growth of dynamically correlated regions is limited only by the system size, implying that confinement effects, usually observed on the scale of tens of particles at most[35], should become relevant macroscopically. On the other hand, temporal fluctuations of the dynamics are suppressed, challenging current views of DH close to jamming and calling for new theories.

*Acknowledgments* We thank L. Berthier for illuminating discussions and M. Cloître for providing us with the samples. This work was partially supported by the European MCRTN “Arrested matter” (MRTN-CT-2003-504712), the NoE “SoftComp” (NMP3-CT-2004-502235), and ACI JC2076 and CNES grants. L.C. is a junior member of the Institut Universitaire de France, whose support is gratefully acknowledged.

*Competing financial interests* The authors declare no competing financial interests.

- 
- [1] Donth, E. *The Glass Transition* (Springer, Berlin, 2001).
- [2] Liu, A. J. & Nagel, S. R. Jamming is not Just Cool Anymore. *Nature* 396, 21 (1998).
- [3] Weeks, E. R., Crocker, J. C., Levitt, A. C., Schofield, A. and Weitz, D. A. Three-dimensional direct imaging of structural relaxation near the colloidal glass transition. *Science* 287, 627-631 (2000).
- [4] Dauchot, O., Marty, G. and Biroli, G. Dynamical heterogeneity close to the jamming transition in a sheared granular material. *Physical Review Letters* 95, 265701 (2005).
- [5] Glotzer, S. C. Spatially heterogeneous dynamics in liquids: insight from simulation. *Journal of Non-Crystalline Solids* 274, 342-355 (2000).
- [6] Ediger, M. D. Spatially heterogeneous dynamics in supercooled liquids. *Annu. Rev. Phys. Chem.* 51, 99-128 (2000).
- [7] Berthier, L. et al. Direct experimental evidence of a growing length scale accompanying the glass transition. *Science* 310, 1797-1800 (2005).
- [8] Keys, A. S., Abate, A. R., Glotzer, S. C. and Durian, D. J. Measurement of growing dynamical length scales and prediction of the jamming transition in a granular material. *Nature Physics* 3, 260-264 (2007).
- [9] Lacevič, N., Starr, F. W., Schroder, T. B., Novikov, V. N. & Glotzer, S. C. Growing correlation length on cooling below the onset of caging in a simulated glass-forming liquid. *Physical Review E* 66, 030101 (2002).
- [10] Biroli G., Bouchaud, J. P., Miyazaki K. & Reichman, D. R. Inhomogeneous mode-coupling theory and growing dynamic length scale in supercooled liquids. *Phys. Rev. Lett.* 97, 195701 (2006)
- [11] Franz, S., Donati, C., Parisi, G. & Glotzer, S. C. On dynamical correlations in supercooled liquids. *Philosophical Magazine B* 79, 1827-1831 (1999).
- [12] Chandler, D., Garrahan, J. P., Jack, R. L., Maibaum, L. & Pan, A. C. Lengthscale dependence of dynamic four-point susceptibilities in glass formers. *Phys. rev. E* 74, 051501 (2006).
- [13] Herk, H. H., Bikoles, N. M., Overgerger, C. G. & Menzes, G. in *Encyclopedia of polymer science and engineering* (ed. al., H. E. M. e.) (Wiley-Interscience, New York, 2003).
- [14] Weitz, D. A. & Pine, D. J. in *Dynamic Light scattering* (ed. Brown, W.) 652-720 (Clarendon

- Press, Oxford, 1993).
- [15] Duri, A., Bissig, H., Trappe, V. & Cipelletti, L. Time-resolved-correlation measurements of temporally heterogeneous dynamics. *Physical Review E* 72, 051401-17 (2005).
  - [16] Measurements in the stationary regime last 50 to 100 times longer than the average relaxation time.
  - [17] Kansal, A. R., Torquato, S. & Stillinger, F. H. Computer generation of dense polydisperse sphere packings. *Journal of Chemical Physics* 117, 8212-8218 (2002).
  - [18] Cipelletti, L., Manley, S., Ball, R. C. & Weitz, D. A. Universal aging features in the restructuring of fractal colloidal gels. *Physical Review Letters* 84, 2275-2278 (2000).
  - [19] Bandyopadhyay, R. et al. Evolution of particle-scale dynamics in an aging clay suspension. *Physical Review Letters* 93, 228302 (2004).
  - [20] Bandyopadhyay, R., Liang, D., Harden, J. L. & Leheny, R. L. Slow dynamics, aging, and glassy rheology in soft and living matter. *Solid State Communications* 139, 589-598 (2006).
  - [21] Knaebel, A. et al. Aging behavior of laponite clay particle suspensions. *Europhys. Lett.* 52, 73 (2000).
  - [22] Chung, B. et al. Microscopic dynamics of recovery in sheared depletion gels. *Physical Review Letters* 96, - (2006).
  - [23] In simulations,  $\chi_4$  is normalized by multiplying the variance of the intermediate scattering function (ISF) —or a similarly-defined correlation function— by the number of particles. Therefore, to compare the order of magnitude of  $\chi$  to that of  $\chi_4$  one should multiply the former by the number of particles in the scattering volume,  $N_p$ , and take the square root, since  $g_2 - 1$  is homogeneous to a squared ISF. For the experiments reported here, the conversion factor is of order  $\sqrt{N_p} \approx 5 \times 10^3$ .
  - [24] Mayer, P. et al. Heterogeneous Dynamics of Coarsening Systems. *Physical Review Letters* 93, 115701 (2004).
  - [25] Weeks, E. R. & Weitz, D. A. Properties of cage rearrangements observed near the colloidal glass transition. *Physical Review Letters* 89 (2002).
  - [26] Marty, G. & Dauchot, O. Subdiffusion and cage effect in a sheared granular material. *Physical Review Letters* 94, 015701 (2005).
  - [27] Reis, P. M., Ingale, R. A. & Shattuck, M. D. Caging Dynamics in a Granular Fluid. *Physical Review Letters* 98, 188301 (2007).



- [28] Brito, C. & Wyart, M. Heterogeneous Dynamics, Marginal Stability and Soft Modes in Hard Sphere Glasses. cond-mat/0611097 (2007).
- [29] Durian, D. J., Pine, D. J. & Weitz, D. A. Multiple light-scattering probes of foam structure and dynamics. *Science* 252, 686-688 (1991).
- [30] Duri, A. & Cipelletti, L. Length scale dependence of dynamical heterogeneity in a colloidal fractal gel. *Europhysics Letters* 76, 972-978 (2006).
- [31] Following ref. [14], one finds  $\sigma_\phi^2 = 2k_0^2\sigma^2\ell/(3\ell^*)$ , where  $k_0$  is the wave vector of the incident light and  $\ell$  is the photon scattering mean free path. For particles much larger than the laser wavelength, as in our case,  $\ell \approx 0.1\ell^*$ , yielding  $\sigma_\phi^2 \approx 20\sigma^2/\mu\text{m}^2$ .
- [32] An additional input parameter is the rearrangement rate per unit volume. However, this parameter only sets the time scale for the simulations with no impact on  $\bar{\beta}$  or  $\chi^*$
- [33] Using a steepest descent method, one can show that for  $1/\sigma_\phi^2 \rightarrow \infty$   $\overline{g_1^{(s)}(\tau)}$  has a compressed exponential shape with a compressing exponent equal to  $p$ . Summing over all paths with different length  $s$  –and thus different decay rates– results in an effective compressing exponent  $\bar{\beta} < p$ .
- [34] Kob, W. & Barrat, J. L. Fluctuations, response and aging dynamics in a simple glass-forming liquid out of equilibrium. *European Physical Journal B* 13, 319 (2000).
- [35] Alcoutlabi, M. & McKenna, G. B. Effects of confinement on material behaviour at the nanometre size scale. *Journal of Physics-Condensed Matter* 17, R461-R524 (2005).

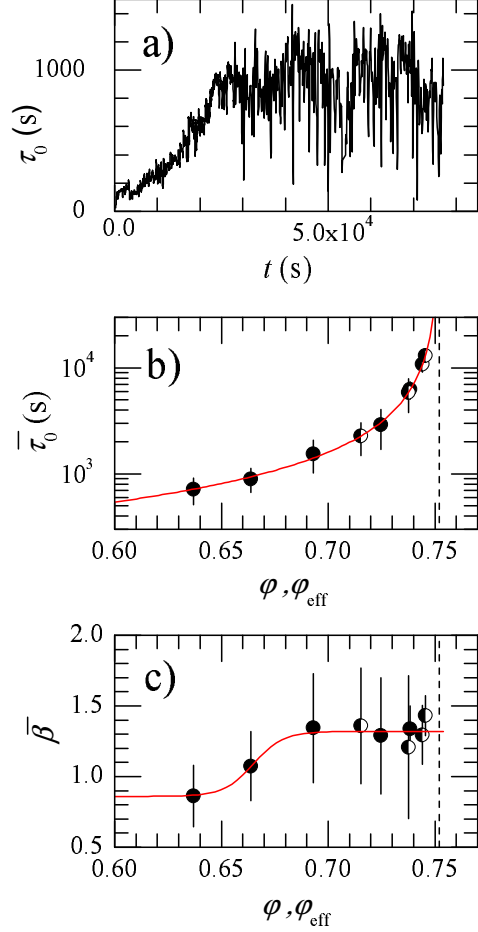


FIG. 1: **Time and volume fraction dependence of the relaxation of concentrated suspensions.**

a) Time dependence of the final relaxation time obtained by fitting the two-time intensity autocorrelation function by a stretched exponential,  $g_2(t, \tau) = a(t) \exp[-(\tau/\tau_0(t))^{\beta(t)}]$ , for a sample at  $\varphi = 0.664$ . After an initial aging regime where the dynamics slows down, the system reaches a dynamically heterogeneous stationary state, where  $\tau_0$  fluctuates significantly without any overall growing trend (the time origin is taken at the end of the sample loading and outgassing). The lower panels show the volume fraction dependence of the relaxation time (b) and the stretching exponent (c) averaged over time in the stationary regime. The solid symbols refer to freshly prepared samples, the semi-filled circles to old samples whose dynamics has been re-initialized. The bars are the standard deviations of the distributions over time of  $\tau_0$  and  $\beta$  in the stationary regime. The solid line in b) is a critical law fit to the growth of  $\tau_0$  for the fresh samples, yielding a critical exponent  $x = 1.01 \pm 0.04$  and a critical packing fraction  $\varphi_{\max} = 0.752$ , indicated by the dashed line here and in c). The solid line in c) is a guide to the eyes.

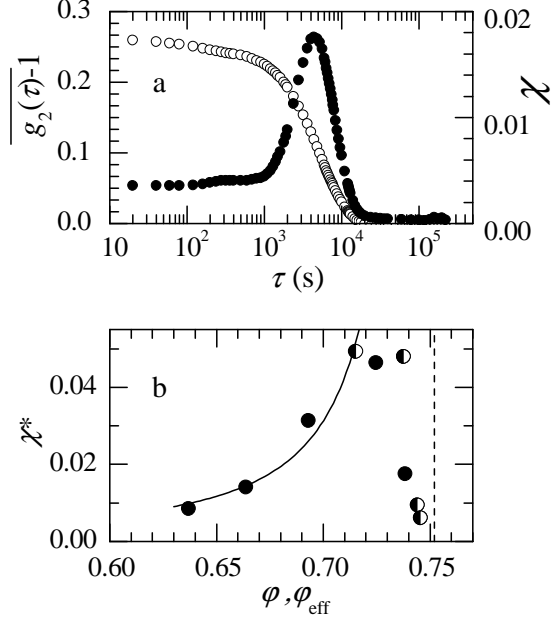


Figure 2; Manuscript NPHYS-2007-05-00481D  
P. Ballesta, A. Duri, and L. Cipelletti

FIG. 2: **Dynamical susceptibility.** a) Average correlation function  $\overline{g_2(\tau)} - 1$  (open symbols and left axis) and dynamical susceptibility (solid symbols and right axis), for a sample at  $\varphi = 0.738$ . b) Volume fraction dependence of the height of the peak of the dynamical susceptibility (same symbols as in Figs. 1b-c). The solid line is a critical-law fit to the initial growth of  $\chi^*$ , yielding an exponent  $y = 1.5 \pm 0.2$ . Note the unexpected drop of  $\chi^*$  near the maximum packing fraction, shown by the dashed line.

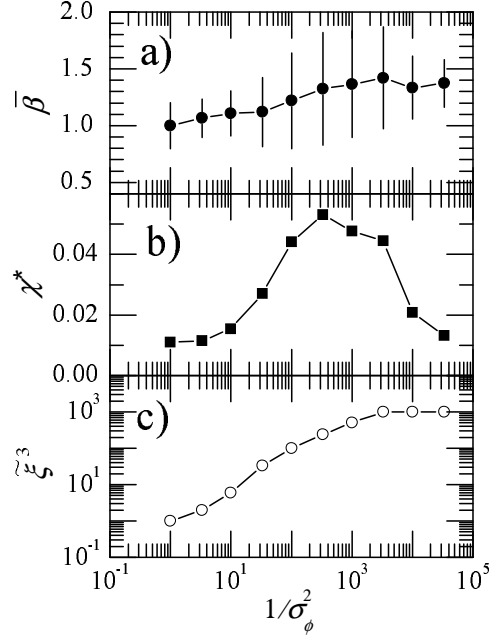


FIG. 3: **Simulations.** Time-averaged stretching exponent  $\bar{\beta}$  (a) and peak of the dynamical susceptibility  $\chi^*$  (b) as a function of  $1/\sigma_\phi^2$ , as obtained from the simulations described in the text (note that  $1/\sigma_\phi^2$  increases with  $\varphi$ ). In a), the bars indicate the standard deviation of the distribution of stretching exponents. The volume  $\tilde{\xi}^3 \equiv (\xi/\ell^*)^3$  of the rearranged regions used as an input in the simulations in order to reproduce the  $\varphi$  dependence of  $\bar{\beta}$  and  $\chi^*$  is shown in (c).  $\xi$  saturates at the value of the smallest dimension of the scattering cell.